

## Nuclear structure and reaction studies with gamma detector arrays at IUAC

R P Singh\*

Inter University Accelerator Centre, New Delhi 110 067, India

Received 3 July 2019

Indian national gamma array (INGA) and gamma detector array (GDA) have been the work horse for nuclear structure studies at IUAC. Many of these studies have revealed a variety of modes of excitations in nuclei as a function of spin, isospin and excitation energy. These excitation modes mirror different underlying symmetries and structures in nuclei for a given mix of above mentioned quantities. Further, there is a rich inter-play between these various modes or degrees of freedom and it's a challenge to experimentally identify and theoretically comprehend the rich spectra exhibited. INGA and GDA setups have also been successfully used in recent years for studying reaction dynamics like incomplete fusion and fusion-fission in heavy ion collisions at energies of about few MeV per nucleon.

**Keywords:** INGA, GDA, High spin, Chirality, Magnetic rotation, Incomplete fusion

### 1 Introduction

Nuclear structure and nuclear reaction studies at Inter university accelerator centre (IUAC) have been carried out using heavy ion accelerators namely, 15 UD Pelletron and a super-conducting linear accelerator LINAC. Typical energies from these accelerators are in the range of 5 to 7 MeV per nucleon and currents of few particle nano-amperes. At present installation and testing of various components to inject beam from an ECR based ion source in to the LINAC is underway. Once the ECR based source is coupled to the LINAC it is expected that higher beam currents and energies would be available for experiments. Gamma detector array (GDA) and Indian national gamma array (INGA)<sup>1</sup> have been used heavily for nuclear structure studies in conjunction with various ancillary devices. In recent years these arrays have also been used for some nuclear reaction studies.

First a brief description of INGA, GDA and some ancillary devices is given followed by some of the studies performed using these arrays.

#### 1.1 Gamma detector array (GDA)

GDA consists of 12, 23% efficiency HPGe detectors placed at a distance of about 20 cm from the target. Each of these detectors is surrounded by an anti compton shield (ACS) detector. ACS detectors are high efficiency scintillator detectors made of NAI(Tl) and BGO crystals. The ACS detectors have a

heavy metal collimator mounted at the front to prevent direct hit from the gamma rays from the target. This combination of ACS-HPGe detectors significantly enables collection of data with significant suppression of compton background. The total photo-peak efficiency of the array is about 0.5 % for a gamma ray of 1 MeV energy. Figure 1(a) shows a picture of the setup in beam hall 1 at IUAC. Four detectors each are placed at three angles 144°, 98° and 50° w.r.t. the beam direction. The setup has been extensively used for probing high spin structure of nuclei populated using pelletron beams with a number of ancillary devices (described briefly later). GDA setup has also been extensively used for study of incomplete fusion reaction at 3-10 MeV per nucleon.

#### 1.2 Indian national gamma array (INGA) at IUAC

INGA is a setup of 24 compton-suppressed clover HPGe detectors. It is part of INGA collaboration of Indian universities and national institutes. In the setup at IUAC the detectors are positioned in six rings at angles of 148°, 123°, 90°, 57° and 32° w.r.t. the beam direction. There are eight detectors at 90° and four each at other angles.

The total solid angle covered by the clover detectors is about 25 percent of 4p and the photo-peak efficiency of the array is about 5% at 1 MeV photon energy. The array is split in to two, the back hemisphere holds 16 and the forward hemisphere holds 8 compton suppressed clover detectors. When the gamma detectors will be used in conjunction with hybrid mass spectrometer (HYRA) the forward array

\*E-mail: rps@iuac.res.in

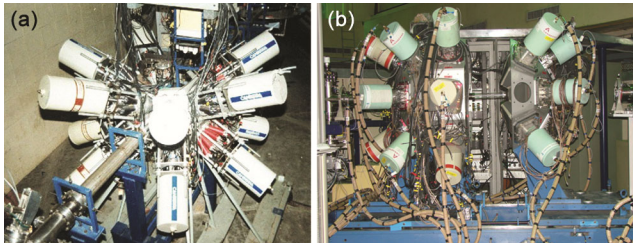


Fig. 1 – (a) Gamma detector array (GDA) and (b) Indian national gamma array (INGA) at IUAC.

would be removed and the backward hemisphere could be moved by about a meter forward to focus on the new target site of HYRA. In Fig. 1(b) a picture of INGA with two hemispheres in opened condition is shown. A number of high density electronics for pulse processing and data acquisition has also been developed at IUAC. Three INGA campaigns have been held so far at IUAC in which several experiments have been done by different research groups from universities and other national and international laboratories.

### 1.3 Ancillary devices

A number of ancillary devices have been used in conjunction with gamma detector arrays to enhance the capability of the system. Some of these are: a 4p phoswich charge particle detector array (CPDA) to detect evaporated light charge particles (alpha, protons) for channel selection, a plunger device for lifetime measurement of excited nuclear states in the sub-nanosecond range and a 14 element BGO multiplicity filter for selecting high spin states. Part of INGA and GDA detectors have also been coupled with mass spectrometer called heavy ion reaction Analyser (HIRA) at IUAC<sup>2</sup> for selection of weak channels based on m/q separation of recoiling residues. Pictures of these devices are shown in Fig. 2. A new plunger device to be used with INGA array was developed and is ready for in-beam test. In recent experiments the CPDA has been used in GDA setup also for incomplete fusion reaction studies.

## 2 Nuclear Structure Studies

GDA and INGA have primarily been used to study the high angular momentum states in nuclei spanning different regions of the periodic table. In recent times there has been significant focus on the study of shape co-existence and various dynamical symmetries in nuclei such as magnetic rotations, chirality and wobbling. Some of these studies are described below:

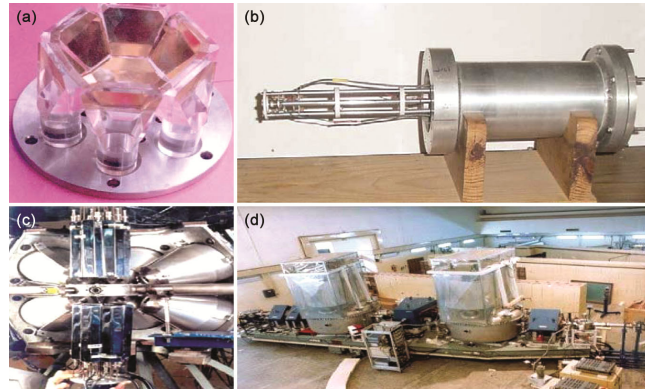


Fig. 2 – (a) Bare one half of a phoswich charge particle detector array with light guides, (b) a plunger device, (c) a 14 element BGO multiplicity filter array and (d) mass spectrometer HIRA at IUAC.

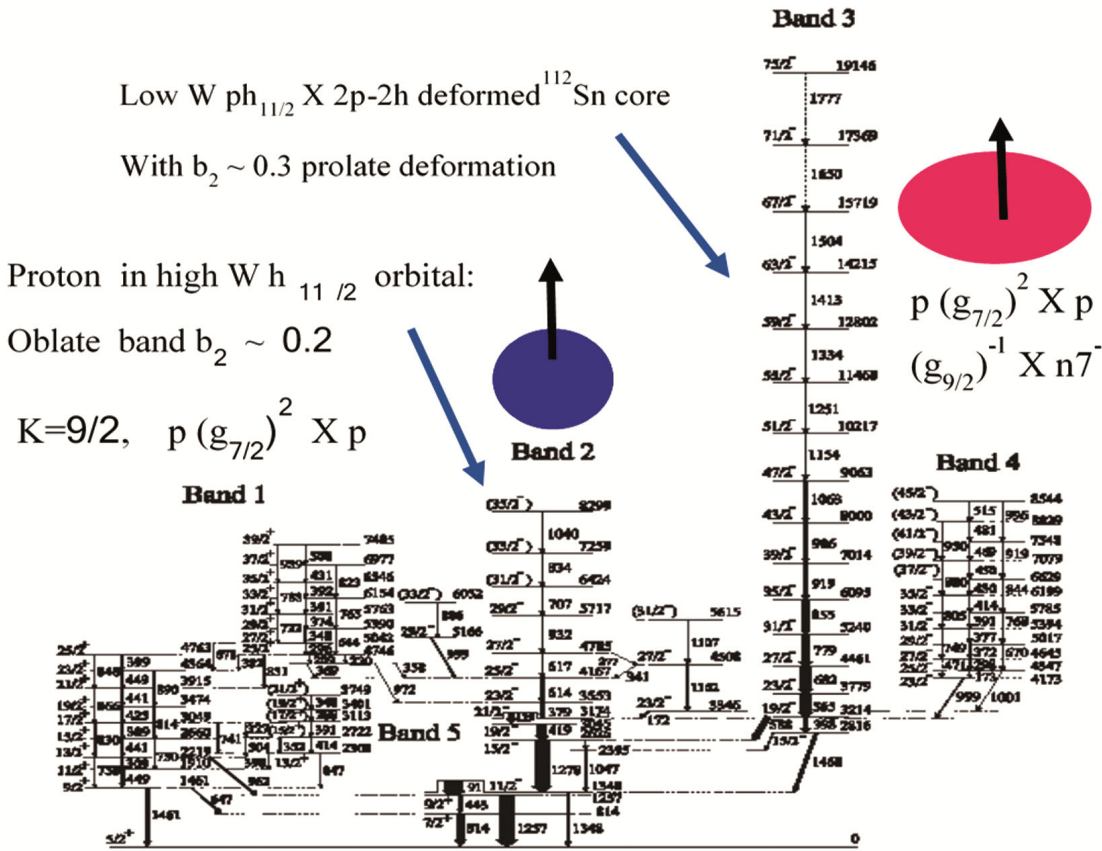
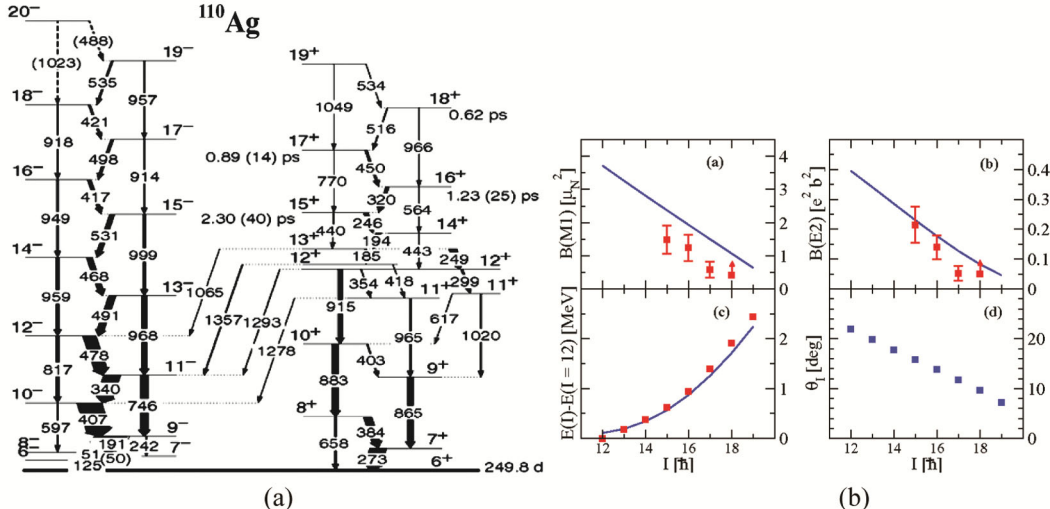
### 2.1 High spin states in $^{113}\text{Sb}$

Nuclei around doubly magic 100 Sn have been of great interest to nuclear physicists. High spin structure of many nuclei in A~100 region have been studied using gamma detector arrays at IUAC, level structure from one such study<sup>3</sup> of  $^{113}\text{Sb}$  is shown in Fig. 3. It could be seen that while the low spin structure is dominated by odd proton coupled to vibrations of  $^{112}\text{Sn}$  core many collective rotational bands develop as the spin and excitation energy increases.

The structure of band 3 was determined to be due to low W  $h_{11/2}$  proton coupled to deformed 2 particle 2 hole core. Based on doppler shifted line shape (DSAM) analysis and total routhian surface (TRS) calculations the band was determined to be of prolate deformation with  $b_2 \sim 0.3$ . Similarly, the structure of band 2 was determined to be high  $\Omega$   $h_{11/2}$  proton coupled to core leading to an oblate deformation with  $b_2 \sim 0.2$ . Band 1 is a strongly coupled band typical of bands with spins aligned close to symmetry axis. Further band 3 showed signatures of band termination at higher spins. Band 4 was another new negative parity highly coupled band with  $\pi(g_{7/2})^2 \times \pi(g_{9/2})^{-1}$   $\times v7^-, v7^-$  represents state of even-even Sn core.

### 2.2 Magnetic rotational bands in A~100

In recent past many experiments in IUAC have focused on probing various aspects of magnetic rotational bands. Such bands arise due to current loops due to valence particles (or holes) in high 'j' orbits coupled almost perpendicular to each other at the band head in nearly spherical nuclei. Figure 4(a) shows magnetic bands from one of our recent study<sup>4</sup> of  $^{110}\text{Ag}$ . In Fig. 4(b) plots for deduced B(M1), B(E2),

Fig. 3 – Partial level scheme of  $^{113}\text{Sb}$ . Adopted from literature<sup>3</sup>Fig. 4 – (a) Partial level scheme of  $^{110}\text{Ag}$  adopted from literature<sup>5</sup> showing negative and positive parity magnetic rotational bands and (b)  $B(\text{M1})$ ,  $B(\text{E2})$ ,  $E(I)-E(I=12)$  along with calculated curves and tilt angle based on shears-principal axis cranking is shown as a function of spin for the positive parity band.

$E(I)-E(I=12)$  along with calculated curves and tilt angle based on shears-principal axis cranking is shown as a function of spin for the positive parity

band. The plots clearly demonstrate success of this model. The negative parity band was already shown to be a case of principal axis cranking.

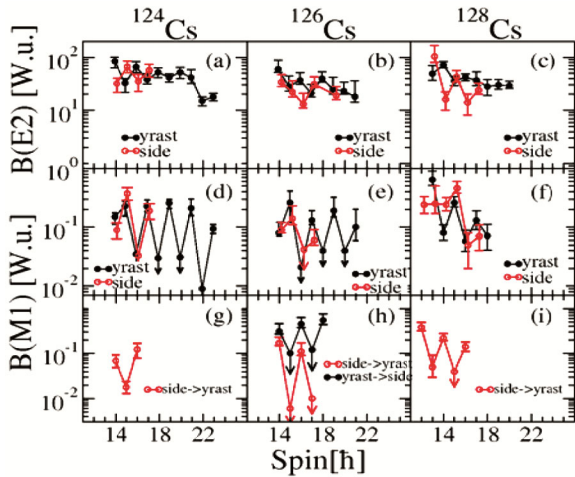


Fig. 5 –  $B(E2)$ ,  $B(M1)$  values as a function of spin for  $^{124}\text{Cs}$ ,  $^{126}\text{Cs}$  and  $^{128}\text{Cs}$  for chiral partner bands from literature<sup>7</sup>.

### 2.3 Chirality in nuclei

Chiral bands observed in nuclei have been one of the two signatures of rigid triaxial shapes in nuclei. A number of nuclei have been investigated for chirality using INGA array. We have measured lifetimes of bands based<sup>5</sup> on  $\pi_{9/2}^- \times \nu h_{11/2}$  in  $^{102}\text{Rh}$  and based on the  $B(E2)$  and  $B(M1)$  values of the transitions we found the bands are not chiral at best they could be due to chiral vibrations. However, lifetime measurements of band based on  $\nu h_{11/2}^- \times nh_{11/2}$  in  $^{124}\text{Cs}$  nucleus revealed the bands to be good chiral partners<sup>6</sup>. Figure 5 shows a comparison of  $B(M1)$  and  $B(E2)$  values for the chiral partner bands.  $B(E2)$  values are very close for the partner bands and  $B(M1)$  values for in-band transitions are in phase while out of phase for intra band transitions as expected for chiral partner bands. For comparison plots for  $^{126}\text{Cs}$  and  $^{128}\text{Cs}$  are also shown for established chiral bands.

### 3 Nuclear Reaction Studies

INGA and GDA setup have also been used for nuclear reaction studies, e.g., fusion-fission dynamics was studied for  $^{16}\text{O} + ^{238}\text{U}$  reaction at 100 MeV using INGA array<sup>7</sup>. In this study fission fragment yields were determined from gamma-gamma coincidence data. GDA setup has been used to characterize incomplete fusion (ICF) reactions at energies of about 3-10 MeV per nucleon for different target projectile combinations. Figure 6 shows a plot of yield at different spins from a recent study<sup>8</sup> for  $^{16}\text{O} + ^{154}\text{Sm}$  at 97.5 MeV reaction. It can be clearly seen that the yield distribution from complete fusion (CF) channels is quite different from that of ICF channels, the yield

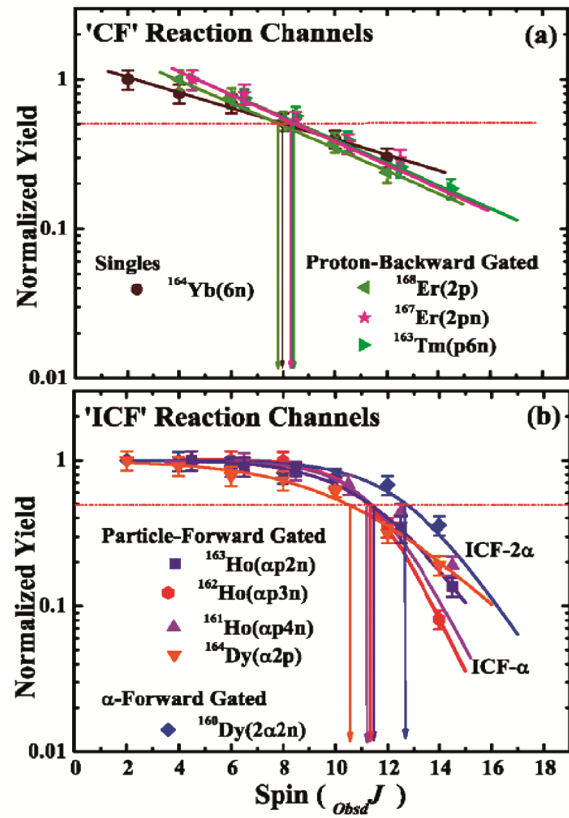


Fig. 6 – Normalized yields as a function of spin for CF and ICF channels obtained after 'p' and 'a' from literature<sup>8</sup>.

for CF channels falls exponentially as a function of spin while that from ICF channels it remains almost constant up to a spin and then falls drastically. The CF and ICF channels were identified by gating on emitted proton and alpha particles at forward and backward angles.

### 4 Summary

INGA and GDA at IUAC have been heavily used for nuclear structure studies at IUAC in conjunction with many ancillary devices. Several interesting problems such as interplay between single particle and collective degrees of freedom in nuclei, shape co-existence and various dynamical symmetries like magnetic rotation and chirality have been studied in the past few years. These arrays have also been effectively used for nuclear reaction studies such as fusion-fission dynamics and incomplete fusion reactions at few MeV per nucleon.

### Acknowledgements

I am indebted to all my colleagues at IUAC, universities, IITs and other research institutions in helping us in the implementation on INGA, GDA

and other setups at IUAC and for their research contributions. I also acknowledge the DST, UGC and DAE for funding INGA and other projects.

## References

- 1 Muralithar S, Rani K, Kumar R, Singh R P, Das J J, Gehlot J, Golda K S, Jhingan A, Madhavan N, Nath S, Sugathan P, Varughese T, Archunan M, Barua P, Gupta A, Jain M, Kothari A, Kumar B P A, Malyadri A J, Naik U G, Kumar Raj, Kumar Rajesh, Zacharias J, Rao S, Saini S K, Suman S K, Kumar M, Subramaniam E T, Venkataraman S, Dhal A, Jnaneswari G, Negi D, Raju M K, Trivedi T & Bhowmik R K, *NIM A*, 622 (2010) 281.
- 2 Sinha A K, Madhavan N, Das J J, Sugathan P, Kataria D O, Patro A P & Mehta G K, *NIM A*, 339 (1994) 543.
- 3 Banerjee P, Ganguly S, Pradhan M K, Sharma H P, Muralithar S, Singh R P & Bhowmik R K, *Phys Rev C*, 87 (2013) 034321.
- 4 Das B, Datta P, Chattopadhyay S, Roy S, Raut R, Bhowmik R K, Goswami A, Jain H C, Kumar R, Muralithar S, Negi D, Pal S, Palit R, & Singh R P, *Phys Rev C*, 98 (2018) 014326.
- 5 Tonev D, Yavahchova M S, Goutev N, Angelis G, Petkov P, Bhowmik R K, Singh R P, Muralithar S, Madhavan N, Kumar R, Raju M K, Kaur J, Mohanty G, Singh A, Kaur N, Garg R, Shukla A, Marinov T K & Brant S, *Phys Rev Lett*, 112 (2013) 052501.
- 6 Selvakumar K, Singh A K, Ghosh C, Singh P, Goswami A, Raut R, Mukherjee A, Datta U, Datta P, Roy S, Gangopadhyay G, Bhowal S, Muralithar S, Kumar R, Singh R P & Raju M K, *Phys Rev C*, 93 (2015) 064307.
- 7 Danu L S, Biswas D C, Saxena A, Shrivastava A, Chatterjee A, Nayak B K, Thomas R G, Choudhury R K, Palit R, Mazumdar I, Datta P, Chattopadhyay S, Pal S, Bhattacharya S, Muralithar S, Golda K S, Bhowmik R K, Das J J, Singh R P, Madhavan N, Gerl J, Patra S K, & Satpathy L, *Phys Rev C*, 81 (2010) 014311.
- 8 Singh D, Linda S B, Giri P K, Mahato A, Tripathi R, Kumar H, Ansari M A, Sathik N P M, Ali R, Kumar R, Muralithar S & Singh R P, *Phys Rev C*, 97 (2018) 064604.